Author Manuscript

Author Manuscript

Author Manuscript

Author Manuscript

HHS Public Access

Author manuscript

Cancer Res. Author manuscript; available in PMC 2015 August 17.

Published in final edited form as:

Cancer Res. 2014 February 15; 74(4): 1227–1237. doi:10.1158/0008-5472.CAN-13-0594.

Loss of Androgen Receptor Expression Promotes a Stem-Like Cell Phenotype in Prostate Cancer through STAT3 Signaling

Anne Schroeder[1,+], **Andreas Herrmann**[2,+], **Gregory Cherryholmes**[2], **Claudia Kowolik**[1], **Ralf Buettner**[1], **Sumanta Pal**[3], **Hua Yu**[2], **Gerhard Müller-Newen**[4,*], and **Richard Jove**[1,*]

[1]Department of Molecular Medicine, Beckman Research Institute and City of Hope Comprehensive Cancer Center, Duarte, CA 91010, USA

[2]Department of Cancer Immunotherapy and Tumor Immunology, Beckman Research Institute and City of Hope Comprehensive Cancer Center, Duarte, CA 91010, USA

[3]Department of Medical Oncology, Beckman Research Institute and City of Hope Comprehensive Cancer Center, Duarte, CA 91010, USA

[4]Institute for Biochemistry, Universitätsklinikum RWTH Aachen, 52074 Aachen, Germany

Abstract

Androgen receptor (AR) signaling is important for prostate cancer progression. However, androgen-deprivation and/or AR targeting-based therapies often lead to resistance. Here we demonstrate that loss of AR expression results in STAT3 activation in prostate cancer cells. AR downregulation further leads to development of prostate cancer stem-like cells (CSC), which requires STAT3. In human prostate tumor tissues, elevated cancer stem-like cell markers coincide with those cells exhibiting high STAT3 activity and low AR expression. AR downregulation-induced STAT3 activation is mediated through increased IL-6 expression. Treating mice with soluble IL-6 receptor fusion protein or silencing STAT3 in tumor cells significantly reduced prostate tumor growth and CSCs. Together, these findings indicate an opposing role of AR and STAT3 in prostate CSC development.

Keywords

STAT3; IL-6; Prostate Cancer; Cancer stem-like cell; AR

INTRODUCTION

Prostate cancer (PC) is the most common cause of male cancer-related deaths in Western countries. Current treatment relies on targeting androgen receptor (AR) signaling by hormone deprivation or anti-androgen therapy. However, tumors are heterogeneous and hormone depletion often results in the selection of drug resistant, highly metastatic tumor cells that survive targeted therapy. Hence, the initial response to treatment is often followed

*Correspondence: rjove@coh.org and mueller-newen@rwth-aachen.de.
+Contributed equally

Notes: The authors declare that they have no conflict of interest.

Author Manuscript Author Manuscript Author Manuscript Author Manuscript

by tumor recurrence (1, 2). The development of recurring PC is not well understood and remains a challenge for more effective therapeutic intervention. Even with new therapies including abiraterone and enzalutamide targeting AR signaling, some cancers do not respond and ultimately recur. One suggested model to explain recurrence proposes the selection of cancer stem-like cells (CSC) that survive drug therapy. Because selected CSCs are thought to be resistant to conventional therapy, and have been suggested to resupply the highly proliferative tumor cell population, failure to eliminate this cell population might result in tumor relapse (3). Cancer cells with stem-cell like properties share phenotypic features with somatic stem cells and are characterized by self-renewal and multilineage differentiation (4). Importantly, the development of CSCs is not well understood and identification of signaling pathways that regulate phenotypic and tumorigenic potential of CSCs might provide new insights for drug development to prevent tumor drug resistance and relapse (5).

Signal Transducer and Activator of Transcription 3 (STAT3) protein has been implicated in maintaining pluripotency and self-renewing processes in embryonic stem cells and glioblastoma stem cells (6–8). STAT3 is a member of the STAT family of transcription factors that transduce signals from cytokine and growth factor receptors on the cell surface and regulate gene expression responses in the nucleus (9). In particular, STAT3 regulates the expression of genes that control cell proliferation, survival and immune responses (10). Persistent activation of STAT3 signaling is oncogenic and has been demonstrated in a wide variety of human tumor specimens and tumor cell lines including leukemias, lymphomas, and a variety of solid tumors such as head and neck cancer, colon, breast and prostate cancer (11–14). Activated STAT3 signaling contributes to oncogenesis by inducing cell proliferation, preventing apoptosis, and suppressing anti-tumor immune responses (15–20). Moreover, constitutive activation of STAT3 has been shown to be important in tumor metastasis and angiogenesis (21–23).

Besides growth factor receptors and non-receptor tyrosine kinases, including EGFR, PDGFR and SRC, activation of STAT3 is mediated by cytokine receptors such as interleukin-6 (IL-6) receptor (9, 24). IL-6 signal transduction is initiated by ligand binding to the IL-6Rα/gp130 receptor complex followed by activation of an intracellular signaling cascade in which receptor-associated Janus Kinases (JAKs) phosphorylate STAT3 on a single tyrosine residue. Upon STAT3 phosphorylation at Y705, STAT3 forms stable dimers and translocates to the nucleus, where it binds to its specific promoter sequences to induce target gene expression (9, 24).

The IL-6/STAT3 signaling pathway has been implicated in the progression of prostate tumors (25). Clinical studies demonstrated elevated levels of IL-6 in blood plasma and blood serum of patients with hormone-refractory prostate cancer (HRPC) or metastatic prostate cancer, compared to benign or non-malignant forms (26, 27). Thus, high IL-6 expression (> 7 pg/ml) has been suggested to participate in malignant progression from hormone-sensitive to hormone-refractory prostate cancer (28). Moreover, IL-6 has been implicated in the maintenance of stem-like cancer cells. In gene expression profiles of $CD44^{+}/CD24^{-}$ breast CSCs, IL-6 has been demonstrated to be upregulated (29). Genetic signatures of prostate CSCs revealed activation of JAK/STAT3 signal transduction in this cell population (30).

Author Manuscript Author Manuscript Author Manuscript Author Manuscript

These observations highlight the IL-6/gp130/STAT3 signaling pathway as a potential target for prostate cancer and PC stem-like cells (31). The IL-6 receptor fusion protein (IL-6^{RFP}) has been described as a cytokine "trap" that efficiently sequesters soluble IL-6 and thereby prevents activation of downstream IL-6 signaling (32–34).

Based on these observations, we investigated the role of activated STAT3 signaling upon androgen blockade on CSC development in PC. Our findings provide new mechanistic insights for PC tumor relapse and CSC development involving STAT3 signaling. We further propose the IL-6 receptor fusion protein (IL-6^{RFP}) as a potential approach to inhibit IL-6/STAT3 signaling and overcome recurrent prostate cancer.

MATERIALS AND METHODS

Cells

Murine epithelial prostate cancer cells TRAMP-C1 (TC1) were obtained originally from American Type Culture Collection (ATCC). TC1- control-, STAT3-, or AR-shRNA engineered cell lines were generated by transducing lentiviral particles containing pLKO1-STAT3 mouse shRNAs (TRCN0000071456), (TRCN0000071453), and (TRCN0000071455) or pLKO1-AR mouse shRNAs (TRCN0000026189), (TRCN0000026195), and (TRCN0000026211) (SIGMA). Pooled populations of transduced cells were used to avoid selection for clonal variants. Cells were cultured in Dulbecco's Modified Eagle Medium (DMEM) medium supplemented with 5% FBS (Gibco, Rockville, MD), 5% Nu-Serum IV, 0.005 mg/ml bovine insulin, 10 nM dehydroisoandrosterone (SIGMA) and 100 U/ml penicillin, 0.1 mg/ml streptomycin (Gibco, Rockville, MD). DU145 cells expressing pLKO1-human STAT3 shRNA (TRCN0000020840) or pLKO1-non-silencing control shRNA were maintained in RPMI supplemented with 10% FBS, 100 U/ml penicillin, 0.1 mg/ml streptomycin, and 2 μg/ml puromycin. Hek293 cells were maintained in DMEM medium supplemented with 10% FBS, 100 U/ml penicillin, 0.1 mg/ml streptomycin. $HEK^{IL\text{-}6RFP}$ cells were stably reconstituted with a cDNA encoding murine IL-6^{RFP} in pcDNA5 FRT/TO using the Flp-In technique (Invitrogen) and selected with Hygromycin (1:100). All cells were obtained before 2008.

In vivo experiments

The Il2-rg(ko)/NOD-SCID mice were kindly provided by Dr. Jun Wu (City of Hope, Duarte, CA). Rag1(ko)Momj/B6.129S7 mice were purchased from Jackson Laboratory. Mouse care and experimental procedures were performed under pathogen-free conditions in accordance with established institutional guidance and approved protocols from the Institutional Animal Care and Use Committee of Beckman Research Institute at City of Hope National Medical Center. Approximately 2–2.5 × 10^6 TC1, TC1 cells expressing non-silencing control-, STAT3-, or AR-shRNA were implanted in mice subcutaneously with HBSS. Palpable tumors were treated peritumorally with either vehicle control (10% EtOH, 90% corn oil), 100 μl flutamide [25 mg/kg] or bicalutamide [50 mg/kg] every other day. 200 μl vehicle control (CM of parental HEK cells) or IL-6^{RFP} [1.8 μg/kg] were injected twice daily. Mice were sacrificed 3–4 weeks after tumor challenge, tumor specimens were harvested and prepared 2 h after last drug treatment for necroptic analysis.

Author Manuscript Author Manuscript Author Manuscript Author Manuscript

Immunofluorescence

For immunofluorescence staining of frozen Matrigel plugs, tissue sections were fixed with 2% paraformaldehyde, permeabilized in methanol, and blocked in PBS supplemented with 10% goat serum and 2.5% mouse serum (Sigma). Sections were incubated overnight with primary antibodies (pYSTAT3, Santa Cruz Biotechnology), AR, Nanog, CD44 (Epitmoics), CD31 (BD-Bioscience), cleaved Caspase3, His (Cell Signaling), Ki67, MSI-1, CD44, Sox-2 (Abcam) diluted 1:50 – 1:100 in PBS containing 10% goat and 2.5% mouse sera. The next day sections were washed with PBS thrice and incubated for 1 h with fluorophore-conjugated secondary antibodies and Hoechst33342 (Invitrogen). Immunofluorescence stainings were analyzed by confocal microscopy (LSM510Meta, Zeiss, Jena, Germany). To acquire mean fluorescence intensities (MFIs), single fluorescence intensities of fluorophore-conjugated secondary antibodies in regions of interest were recorded by total fluorescence per field of view in a 12 bit mode and relative units were quantified and averaged.

Archival human prostate carcinoma tissues from an anonymous group of patients were provided by the Pathology Core of City of Hope Comprehensive Cancer Center. Tumor tissues were formalin fixed and paraffin embedded. Sections of 3 μm were deparaffinized, and processed as described above. These sections were stained with antibodies raised against pYSTAT3 (1:50 Santa Cruz Biotechnology), AR (1:50 Epitomics), MSI-1 (1:50 Ebioscience), Sox2, Nanog, CD44, integrin α2β1 (1:50 Abcam), and secondary antibodies conjugated to fluorophores diluted 1:100 (Invitrogen), additionally incubated with Hoechst33342 (Invitrogen), then mounted with Mowiol and analyzed by confocal microscopy.

Intravital multiphoton microscopy (IVMPM)

Mice were anesthetized with an isoflurane/oxygen gas, and prepared for surgery. Then mice were injected with 100 μg dextran-rhodamine and 25 μg of Hoechst33342 (Invitrogen) intravenously. Tumor bearing mice continued to receive isofluorane/oxygene anesthesia while 2-photon live imaging was performed using Prairie Technologies Ultima microscope (Middleton, WI). To record rhodamine, signals were measured at λ[excit] = 860 nm with emission between 565 nm – 615 nm (rhodamine). For recording Hoechst33342, emission signals were recorded at λ[excit] = 730 nm with emission between 435 nm – 485 nm. Extracellular matrix (ECM) emission was given by second harmonic generation at λ[excit] = 890 nm (Coherent Chameleon Ultra II Ti:Sa laser). Images were acquired using an Ultima Multiphoton Microscopy System (Prairie Technologies) equipped with Prairie View software and non-descanned Hamamatsu PhotoMultiplier Tubes. Images were collected in 512×512 pixels, 16-bit resolution. TIFF formatted images were analyzed by Image Pro Plus professional imaging software (Media Cybernetics, Bethesda, MD).

Western blot analysis

Cell lysates were prepared and protein concentrations were determined by Bio-Rad protein assay. Equivalent amounts of total proteins were separated by 10% SDS-PAGE (Invitrogen), subjected to immunoblotting, probed with the respective antibodies, and detected for signals using horseradish peroxidase–conjugated secondary antibodies by enhanced chemiluminescence (Amersham).

Author Manuscript Author Manuscript Author Manuscript Author Manuscript

Tumor sphere formation

Cells were resuspended and dissociated into single cells by using a 40 μm cell strainer. To remove remaining serum, cells were washed thrice with HBSS (Invitrogen). Then, tumor cells were resuspended in 3 ml TSM consisting of DMEM F-12, L-Glutamine (1%), 1M Hepes (2.5%), B-27 (50X), Heparin Sodium, and plated at a density of 4×10^4 cells/6-well plate. 20 ng/ml FGF-2 and EGF were added freshly. Tumor spheres with at least 20 cells per sphere were counted every other day using a transmitted light microscope for six days.

RESULTS

Loss of AR expression activates STAT3 signaling in prostate cancer cells

Treatment with anti-androgens is one of the standard therapies for androgen-sensitive prostate cancer. Development of androgen-insensitivity is the major obstacle for therapeutic intervention in recurrent prostate cancer. To determine the role of STAT3 in the transition from androgen-sensitive to hormone-refractory prostate cancer upon hormone deprivation, mice bearing TC1 murine prostate tumors derived from TRAMP transgenic mice were treated with the AR antagonist flutamide. TC1 cells implanted *s.c.* into Rag1−/− mice, established tumors within four weeks after implantation and expressed AR. Treatment with flutamide resulted in an immediate growth suppression (fig. 1A, F_I). However, repeated flutamide administration did not result in tumor rejection, but rather continued tumor growth (fig. 1A, F_{II}). Compared to vehicle treated control, AR expression was significantly decreased at the onset of flutamide administration (fig. 1B, F_I; fig. 1C, F_I) as well as in advanced tumor growth (fig. 1B, F_{II}; fig. 1C, F_{II}). By contrast, STAT3 expression and activation significantly increased in TC1 tumors challenged with flutamide, as shown by Western blot analysis and immunofluorescence staining (fig. 1B, F_I F_{II}; fig. 1C, F_I F_{II}).

Using RNAi approaches to silence either AR or STAT3 expression in prostate cancer cells, tumor growth kinetics of engrafted engineered cells indicate that STAT3 knockdown delays tumor growth significantly (fig. 1D). Conversely, silencing AR expression had no effect on tumor growth (fig. 1D), tumor vasculature (fig. S1A), or proliferative activity (fig. S1B). Furthermore, AR knockdown resulted in a more robust STAT3 activation, suggesting that STAT3 signaling compensates for silenced AR and promotes tumor growth (fig. 1E). In all RNAi experiments, pooled populations of transduced cells were used to avoid selection of clonal variants and RNAi specificity was validated. Hence, downregulation of AR signaling achieved either by antagonizing AR with flutamide or silencing AR expression through RNAi is accompanied by enhanced STAT3 activity, thereby favoring disease progression and tumor growth. Correspondingly, AR mRNA expression is significantly decreased in association with enhanced STAT3 activity in TC2 murine prostate cancer cells (fig. S1C). TC2 cells are considered to represent more advanced prostate cancer than TC1 cells, which is reflected by significantly improved tumor growth (fig. S1D) and elevated expression of Ras and Myc similar to high-grade human prostate cancer (fig. S1E).

Author Manuscript Author Manuscript Author Manuscript Author Manuscript

AR downregulation-associated STAT3 activation promotes the development of prostate CSCs

Because enhanced STAT3 activity in cancer cells has been suggested to impact the tumorigenic potential by unbalancing differentiation and promoting the expansion of cancer stem-like cells, we analyzed the potential of STAT3 and AR to induce a CSC phenotype. Antagonizing AR in murine prostate tumors with flutamide resulted in significantly elevated protein expression of Musashi-1, Sox2, and CD44 (fig. 2A). Furthermore, AR silencing promoted tumor sphere formation of prostate cancer cells (fig. 2B, left panel), associated with increased STAT3 activity as well as increased expression of Musashi-1 and Sox2 (fig. 2B, right panel). Thus, AR inhibition selected for a shift from $AR^{+}/pSTAT3^{-}/MSI^{-}/Sox2^{-}$ expression to a cancer cell stem-like phenotype with $AR^{-}/pSTAT3^{+}/MSI^{+}/Sox2^{+}$ expression as seen both *in vitro* and *in vivo* (fig. 2C). In striking contrast, genetic silencing of STAT3 suppressed tumor sphere formation significantly, concomitant with reduction of CSC marker expression (fig. 2B and C). This indicates that AR signaling downregulation, achieved by either androgen antagonists or genetic silencing, favors STAT3 activity and consequently expression of CSC markers leading to the induction of a prostate CSC phenotype. As shown in figure 2D, AR is not associated with CD44 expression (upper panel), while $pSTAT3^{+}/CD44^{+}$ expressing cells represent the major population (lower panel) in untreated prostate tumors. Hence, reduced AR activity promotes the CSC phenotype at least in part through activation of STAT3.

Human prostate CSCs are characterized by low AR and high p-STAT3 levels

To elucidate the role of STAT3 activity in mounting the CSC repertoire resulting in sustained malignacy of human prostate tumors, we investigated the co-expression of STAT3 and AR with CD44, which is thought to impact tumor initiation as well as homing/metastasis to the bone marrow, and Sox2 and integrin $\alpha2\beta1$, both of which are involved in self-renewal. As shown by analysis of patient biopsies, activated STAT3 is associated predominantly with elevated Sox2 and integrin $\alpha2\beta1$ expression (fig. 3A), as well as with CD44, Musashi-1, and Nanog expression (fig. S2AB). In contrast, lack of pSTAT3 is associated with substantially decreased expression of Sox2 and integrin $\alpha2\beta1$. Notably, pSTAT3 does not coincide with AR expression (fig. 3B). Accordingly, CD44 or Sox2 protein expression is not accompanied by AR expression, which is instead expressed locally constrained and excluded from $CD44^{+}$ or $Sox2^{+}$ cell clusters (fig. 3C). Thus, $Sox2^{+}$ human CSCs of the prostate characteristically express elevated pSTAT3 but not AR (fig. 3D, fig. S2B), which emphasizes a critical role for STAT3 in tumor progression.

Blocking IL-6/STAT3 signaling inhibits development of prostate CSCs

Since IL-6 mRNA expression was elevated in AR-targeted tumors by either anti-androgen or silencing of AR (fig. 4A), we evaluated the role of IL-6 as a potential mediator of STAT3 activation in prostate CSCs. We employed the IL-6 cytokine "trap" $IL\text{-}6^{RFP}$, a soluble fusion protein of the ligand-binding domains of the IL-6 receptor subunits gp130 and IL-6Rα (32). *In vitro* characterization of $IL\text{-}6^{RFP}$ verified IL-6 binding capability and IL-6 neutralizing activity in prostate cancer cells (fig. S3A–G). Although systemic *in vivo* delivery of $IL\text{-}6^{RFP}$ induces a significant delay in tumor growth kinetics, local administration of $IL\text{-}6^{RFP}$ shows

Author Manuscript Author Manuscript Author Manuscript Author Manuscript

an improved anti-tumoral efficacy early on (fig. S3H). Most importantly, comparison of mice treated with equimolar concentrations of IL-6^{RFP} or anti-IL-6 antibodies revealed that antitumoral efficacy of IL-6^{RFP} is improved by 3-fold over anti-IL-6 antibodies (fig. 4B and S3I). Moreover, compared to anti-IL-6 cytokine depletion antibodies, IL-6^{RFP} driven inhibition of STAT3 signaling is considerably enhanced (3.5 fold) (fig. S3G).

In murine 3D cell culture *in vitro*, we evaluated the maturation of CD44^{+}/Sox2^{+} tumor spheres upon IL-6^{RFP} treatment, which resulted in decreased sphere formation and STAT3 activity (fig. S3J). Therefore, we assessed the therapeutic efficacy of blocking IL-6 signaling by administering IL-6^{RFP} *in vivo* and targeting the "stemness" phenotype in prostate cancer. Treatment with IL-6^{RFP} resulted in significantly reduced STAT3 activity, concomitant with decreased protein expression levels of MSI-1, Sox2, CD44, and Nanog (fig. 4CDE, fig. S3JK).

As shown by immunofluorescence staining of tumor microsections, the phosphorylation of STAT3 (fig. 4D) and expression of stem cell markers, such as MSI-1 and Nanog (fig. 4E, fig. S3K), is locally inhibited by tumor permeating IL-6^{RFP}. This finding indicates that blocking IL-6 mediated STAT3 signaling prevents maturation of multipotent CSC populations by inhibiting the expression of critical "stemness" regulators. Moreover, the regenerative potential of human prostate CSCs was considerably reduced after blocking IL-6/STAT3 signaling by IL-6^{RFP}. Human tumor sphere formation was significantly inhibited, accompanied by diminished expression of pSTAT3, MSI-1, and Sox2 (fig. 4F). As anticipated from rodent prostate cancer stem-like cell populations, the presence of STAT3 is essential to mediate the expression of human CSC markers such as MSI-1 and Sox2, as well as triggering tumor sphere formation as shown by STAT3 knockdown assays (fig. 4G). We confirmed these findings by treating human DU145 tumors with IL-6^{RFP} resulting in significant tumor growth delay (fig. 4H). Tumor permeating IL-6^{RFP} efficiently inhibited STAT3 activation (fig. 4IJ) and led to dramatically reduced expression of Sox2 and MSI-1 as shown by Western blot analysis from tumor homogenates (fig. 4K). Thus, blocking IL-6/STAT3 signaling substantially diminishes the CSC phenotype in the prostate.

Targeting both IL-6/STAT3 and AR signaling pathways gives stronger anti-tumor effects

Both therapeutic interventions, androgen depletion and inhibition of IL-6 triggered STAT3 signaling, exert anti-tumor activity as monotherapy. Furthermore, silencing IL-6/STAT3 signaling prevents prostate CSC maturation. Therefore we combined the clinically more relevant anti-androgen, bicalutamide, and IL-6^{RFP} treatments to assess their combined potential for therapeutic benefit. Combinatorial therapy significantly reduced tumor growth but showed only slightly improved anti-tumor efficiency compared to treatment with IL-6^{RFP} alone, while anti-androgen administration alone had a minor effect on tumor growth kinetics (fig. 5A) Tumors treated with IL-6^{RFP} alone or in combination with bicalutamide were positive for apoptotic cell death associated with downregulation of Bcl-2 and Bcl$_{XL}$ (fig. 5B), and exhibited a significant decrease in proliferative activity as shown by Ki67^{+} staining (fig. 5C). Interestingly, androgen-depletion alone led to accumulation of a CD44^{+} cell population in the tumor, as shown by 2-photon imaging *in vivo* (fig. 5D). This indicates that bicalutamide treatment contributes to undesired CD44 expression suggestive of CSC

Author Manuscript Author Manuscript Author Manuscript Author Manuscript

development in prostate tumor tissue. By contrast, combination with IL-6^{RFP} or IL-6^{RFP} treatment alone resulted in significantly decreased amounts of CD44^{+} cells (fig. 5D). Importantly, while bicalutamide administration alone had no beneficial effect on CSC marker expression, combined androgen depletion and IL-6^{RFP} treatment enhanced suppression of MSI-1 and Sox2 expression (fig. 5E).

DISCUSSION

Standard treatment for prostate cancer targets the AR signaling pathway. However, therapeutic intervention often results in tumor relapse due to drug resistance and mechanistic explanations for this failure are diverse. A model based on the presence of prostate CSCs that are selected for drug resistance and allow sustained tumor progression could provide an explanation (35). Nevertheless, the underlying mechanisms for development of CSCs are not well understood. The cell populations initiating tumor growth and driving tumor relapse as a consequence of conventional therapies remain undefined. It has been suggested that CSCs may derive from somatic stem cells, progenitor or differentiated cells as well as highly proliferative, differentiated cancer cells by genetic or tumor microenvironment alterations (4). In these models, CSCs have been proposed to induce tumor growth and differentiate into the various cell types within a tumor. For the identification of CSCs, several markers have been suggested including Sox2, Nanog, CD44, integrin α2β1, and MSI-1 (36–38).

Here, we mainly use murine tumor cells derived from transgenic spontaneous adenocarcinoma of the mouse prostate (TRAMP) model, which are of luminal origin, mirror primary PC (39) and express AR and STAT3. We demonstrate that chemotherapeutic intervention targeting the AR signaling pathway, which is important for differentiation and survival, promotes the development of a CSC phenotype and that this may, at least in part, be responsible for tumor relapse. Our data further indicate that inhibition of AR by either anti-androgens or gene-silencing results in up-regulation of the IL-6 cytokine (fig. 4A). While anti-androgen slows tumor growth more effectively than AR knockdown, this may reflect a delay in elevated IL-6 induction by anti-androgen treatment. Importantly, IL-6 induced activation of STAT3 signal transduction coincides with augmented CSC marker expression. We show that lack of AR is associated with this elevated STAT3 activity and augmented expression of CSC markers. In particular, AR-negative tumor cells exhibited increased MSI-1, Sox2 and CD44 expression, which was associated with activated STAT3 signaling. In human prostate cancer tissues, elevated CSC markers coincided with those cells exhibiting high STAT3 activity and low AR expression, indicating an inverse correlation between AR and pSTAT3 expression in the maturation of CSC in human prostate cancer progression. This counter-regulation of the AR and STAT3 signaling pathways in both mouse and human tumor cells provides a potential explanation for failure of mono-therapies inhibiting the AR signaling pathway.

To effectively target the maturation of CSCs in prostate cancer, we applied a chimeric soluble IL-6 receptor fusion protein (IL-6^{RFP}) with improved inhibitory activity compared to IL-6 depletion antibodies. Inhibition of the STAT3 signaling pathway by gene silencing or using IL-6^{RFP} in murine and human prostate cancer cells resulted in decreased CSC phenotype development *in vitro* and *in vivo*. Moreover, IL-6^{RFP} positive areas in tumor

Author Manuscript Author Manuscript Author Manuscript Author Manuscript

tissue revealed specific reduction of CSC markers including MSI-1 and Nanog, suggesting that STAT3 activity is directly associated with CSC marker expression. Recent studies imply the IL-6 cytokine to be essential to enter senescence (40, 41) and subsequently maintain de-differentiation/pluripotency (42). This is consistent with studies in glioblastoma showing that inhibition of the IL-6Rα expression diminished STAT3 activation, which was associated with reduced tumor growth and numbers of glioblastoma stem cells (7). Our data are consistent with and further expand on the studies of Wicha *et al.* (43). Although previous studies have suggested that prostate CSCs are AR negative (44, 45), our findings indicate IL-6 secretion and downstream STAT3 mediated signaling as a critical pathway after blockade of AR, thereby maintaining potential towards development of the CSC phenotype as well as initiating tumorigenic progression.

The efficacy of targeting CSCs is often hampered by drug resistance, which is a challenge for therapeutic intervention using small-molecule drugs that exert their inhibitory activity intracellularly. Previous studies have demonstrated elevated levels of proteins exerting multi-drug resistance such as ABCB1 and ABCG2 (46). Hence, inhibiting IL-6 with the IL-6^{RFP} has several attractive aspects for targeting CSCs. Depletion of IL-6 is thought to impact the induction of cell senescence, which is considered one of the initial steps in the transition to a CSC phenotype (41). Blocking IL-6 would inhibit STAT3-mediated IL-6 signaling, which maintains the CSC phenotype, and downregulate STAT3 target gene induction such as Bcl-xL, Survivin, and c-Myc. Finally, IL-6 signaling repression is thought to negatively impact IL-6R-mediated MAPK signaling and PI3K signaling. The PI3K pathway is deregulated in many human tumors including prostate cancer and inhibition revealed promising results in cancer therapy (47). Therefore, our data suggest that IL-6^{RFP} or similar strategies are promising therapeutic agents for PC to reduce tumor growth and prevent recurring PC by targeting the CSC population.

It is unlikely that mono-therapies targeting the IL-6/STAT3 signaling pathway will be effective for complete tumor rejection. It has been shown that first-line treatment inhibiting AR results in tumor regression, since the tumor bulk is eliminated. However, it seems possible that AR^{-}/$pSTAT3^{+}$ expressing CSCs can survive and differentiate into AR-dependent tumor cells even with low levels of androgens. Thus, targeting the tumor bulk with an AR inhibitor and at the same time preventing the de-differentiated CSC cell population with high STAT3 activity is likely advantageous. Combining inhibition of IL-6/STAT3 with androgen blockade resulted in improved therapeutic benefit compared to the respective mono-therapies. Importantly, IL-6 inhibition by IL-6^{RFP} prevails over the anti-androgen induced CSC phenotype development. Hence, our data support the concept that combination of AR and STAT3 inhibitors may be the most effective PC therapy. A similar reciprocal regulation between AR and PI3K signaling has been found in *Pten*-deficient mice (48).

In summary, our results demonstrate that blockade of AR mediates activation of STAT3 signaling through up-regulation of IL-6, which is associated with the development of a CSC phenotype. Conversely, inhibition of the IL-6/STAT3 signaling pathway with IL-6 receptor fusion protein diminishes the CSC population, which results in reduced tumor growth. These findings provide new mechanistic insight into the emergence of drug resistant prostate

Author Manuscript Author Manuscript Author Manuscript Author Manuscript

cancer. Moreover, combination of IL-6^{RFP} and anti-androgens inhibited CSCs and differentiated AR-positive cancer cells, and therefore provides a promising treatment of PC to prevent eventual tumor relapse.

Supplementary Material

Refer to Web version on PubMed Central for supplementary material.

Acknowledgments

We thank Dr. Cy Stein, Dr. Jeremy Jones, Dr. Tommy Tong and members of our laboratories for valuable comments and discussion. This work was supported by NCI grant R01 CA115674 (RJ) and by the Beckman Research Institute at City of Hope Comprehensive Cancer Center.

References

1. Feldman BJ, Feldman D. The development of androgen-independent prostate cancer. Nat Rev Cancer. 2001; 1:34–45. [PubMed: 11900250]
2. Singh P, Yam M, Russell PJ, Khatri A. Molecular and traditional chemotherapy: a united front against prostate cancer. Cancer Lett. 2010; 293:1–14. [PubMed: 20117879]
3. Maitland NJ, Collins AT. Prostate cancer stem cells: a new target for therapy. J Clin Oncol. 2008; 26:2862–70. [PubMed: 18539965]
4. Magee JA, Piskounova E, Morrison SJ. Cancer stem cells: impact, heterogeneity, and uncertainty. Cancer Cell. 2012; 21:283–96. [PubMed: 22439924]
5. Dalerba P, Cho RW, Clarke MF. Cancer stem cells: models and concepts. Annu Rev Med. 2007; 58:267–84. [PubMed: 17002552]
6. Raz R, Lee CK, Cannizzaro LA, d'Eustachio P, Levy DE. Essential role of STAT3 for embryonic stem cell pluripotency. Proc Natl Acad Sci U S A. 1999; 96:2846–51. [PubMed: 10077599]
7. Wang H, Lathia JD, Wu Q, Wang J, Li Z, Heddleston JM, et al. Targeting interleukin 6 signaling suppresses glioma stem cell survival and tumor growth. Stem Cells. 2009; 27:2393–404. [PubMed: 19658188]
8. Sherry MM, Reeves A, Wu JK, Cochran BH. STAT3 is required for proliferation and maintenance of multipotency in glioblastoma stem cells. Stem Cells. 2009; 27:2383–92. [PubMed: 19658181]
9. Darnell JE Jr, Kerr IM, Stark GR. Jak-STAT pathways and transcriptional activation in response to IFNs and other extracellular signaling proteins. Science. 1994; 264:1415–21. [PubMed: 8197455]
10. Yu H, Pardoll D, Jove R. STATs in cancer inflammation and immunity: a leading role for STAT3. Nat Rev Cancer. 2009; 9:798–809. [PubMed: 19851315]
11. Yu H, Jove R. The STATs of cancer--new molecular targets come of age. Nat Rev Cancer. 2004; 4:97–105. [PubMed: 14964307]
12. Bromberg JF, Wrzeszczynska MH, Devgan G, Zhao Y, Pestell RG, Albanese C, et al. Stat3 as an oncogene. Cell. 1999; 98:295–303. [PubMed: 10458605]
13. Catlett-Falcone R, Landowski TH, Oshiro MM, Turkson J, Levitzki A, Savino R, et al. Constitutive activation of Stat3 signaling confers resistance to apoptosis in human U266 myeloma cells. Immunity. 1999; 10:105–15. [PubMed: 10023775]
14. Sen M, Thomas SM, Kim S, Yeh JI, Ferris RL, Johnson JT, et al. First-in-human trial of a STAT3 decoy oligonucleotide in head and neck tumors: implications for cancer therapy. Cancer Discov. 2012; 2:694–705. [PubMed: 22719020]
15. Masuda M, Suzui M, Yasumatu R, Nakashima T, Kuratomi Y, Azuma K, et al. Constitutive activation of signal transducers and activators of transcription 3 correlates with cyclin D1 overexpression and may provide a novel prognostic marker in head and neck squamous cell carcinoma. Cancer Res. 2002; 62:3351–5. [PubMed: 12067972]

Author Manuscript Author Manuscript Author Manuscript Author Manuscript

16. Ramana CV, Grammatikakis N, Chernov M, Nguyen H, Goh KC, Williams BR, et al. Regulation of c-myc expression by IFN-gamma through Stat1-dependent and -independent pathways. EMBO J. 2000; 19:263–72. [PubMed: 10637230]
17. Bowman T, Garcia R, Turkson J, Jove R. STATs in oncogenesis. Oncogene. 2000; 19:2474–88. [PubMed: 10851046]
18. Li N, Grivennikov SI, Karin M. The unholy trinity: inflammation, cytokines, and STAT3 shape the cancer microenvironment. Cancer Cell. 2011; 19:429–31. [PubMed: 21481782]
19. Yu H, Kortylewski M, Pardoll D. Crosstalk between cancer and immune cells: role of STAT3 in the tumour microenvironment. Nat Rev Immunol. 2007; 7:41–51. [PubMed: 17186030]
20. Lo HW, Hsu SC, Xia W, Cao X, Shih JY, Wei Y, et al. Epidermal growth factor receptor cooperates with signal transducer and activator of transcription 3 to induce epithelial-mesenchymal transition in cancer cells via up-regulation of TWIST gene expression. Cancer Res. 2007; 67:9066–76. [PubMed: 17909010]
21. Dechow TN, Pedranzini L, Leitch A, Leslie K, Gerald WL, Linkov I, et al. Requirement of matrix metalloproteinase-9 for the transformation of human mammary epithelial cells by Stat3-C. Proc Natl Acad Sci U S A. 2004; 101:10602–7. [PubMed: 15249664]
22. Xie TX, Wei D, Liu M, Gao AC, Ali-Osman F, Sawaya R, et al. Stat3 activation regulates the expression of matrix metalloproteinase-2 and tumor invasion and metastasis. Oncogene. 2004; 23:3550–60. [PubMed: 15116091]
23. Xu Q, Briggs J, Park S, Niu G, Kortylewski M, Zhang S, et al. Targeting Stat3 blocks both HIF-1 and VEGF expression induced by multiple oncogenic growth signaling pathways. Oncogene. 2005; 24:5552–60. [PubMed: 16007214]
24. Heinrich PC, Behrmann I, Haan S, Hermanns HM, Muller-Newen G, Schaper F. Principles of interleukin (IL)-6-type cytokine signalling and its regulation. Biochem J. 2003; 374:1–20. [PubMed: 12773095]
25. Culig Z, Puhr M. Interleukin-6: a multifunctional targetable cytokine in human prostate cancer. Mol Cell Endocrinol. 2012; 360:52–8. [PubMed: 21664423]
26. Adler HL, McCurdy MA, Kattan MW, Timme TL, Scardino PT, Thompson TC. Elevated levels of circulating interleukin-6 and transforming growth factor-beta1 in patients with metastatic prostatic carcinoma. J Urol. 1999; 161:182–7. [PubMed: 10037394]
27. Akimoto S, Okumura A, Fuse H. Relationship between serum levels of interleukin-6, tumor necrosis factor-alpha and bone turnover markers in prostate cancer patients. Endocr J. 1998; 45:183–9. [PubMed: 9700471]
28. Nakashima J, Tachibana M, Horiguchi Y, Oya M, Ohigashi T, Asakura H, et al. Serum interleukin 6 as a prognostic factor in patients with prostate cancer. Clin Cancer Res. 2000; 6:2702–6. [PubMed: 10914713]
29. Marotta LL, Almendro V, Marusyk A, Shipitsin M, Schemme J, Walker SR, et al. The JAK2/STAT3 signaling pathway is required for growth of CD44(+)CD24(−) stem cell-like breast cancer cells in human tumors. J Clin Invest. 2011; 121:2723–35. [PubMed: 21633165]
30. Birnie R, Bryce SD, Roome C, Dussupt V, Droop A, Lang SH, et al. Gene expression profiling of human prostate cancer stem cells reveals a pro-inflammatory phenotype and the importance of extracellular matrix interactions. Genome Biol. 2008; 9:R83. [PubMed: 18492237]
31. Hellsten R, Johansson M, Dahlman A, Sterner O, Bjartell A. Galiellalactone inhibits stem cell-like ALDH-positive prostate cancer cells. PLoS One. 2011; 6:e22118. [PubMed: 21779382]
32. Wiesinger MY, Haan S, Wuller S, Kauffmann ME, Recker T, Kuster A, et al. Development of an IL-6 inhibitor based on the functional analysis of murine IL-6Ralpha(1). Chem Biol. 2009; 16:783–94. [PubMed: 19635415]
33. Metz S, Wiesinger M, Vogt M, Lauks H, Schmalzing G, Heinrich PC, et al. Characterization of the Interleukin (IL)-6 Inhibitor IL-6-RFP: fused receptor domains act as high affinity cytokine-binding proteins. J Biol Chem. 2007; 282:1238–48. [PubMed: 17085445]
34. Ancey C, Kuster A, Haan S, Herrmann A, Heinrich PC, Muller-Newen G. A fusion protein of the gp130 and interleukin-6Ralpha ligand-binding domains acts as a potent interleukin-6 inhibitor. J Biol Chem. 2003; 278:16968–72. [PubMed: 12646580]

Author Manuscript Author Manuscript Author Manuscript Author Manuscript

35. Collins AT, Maitland NJ. Prostate cancer stem cells. Eur J Cancer. 2006; 42:1213–8. [PubMed: 16632344]
36. Collins AT, Berry PA, Hyde C, Stower MJ, Maitland NJ. Prospective identification of tumorigenic prostate cancer stem cells. Cancer Res. 2005; 65:10946–51. [PubMed: 16322242]
37. Gu G, Yuan J, Wills M, Kasper S. Prostate cancer cells with stem cell characteristics reconstitute the original human tumor in vivo. Cancer Res. 2007; 67:4807–15. [PubMed: 17510410]
38. Wang XY, Penalva LO, Yuan H, Linnoila RI, Lu J, Okano H, et al. Musashi1 regulates breast tumor cell proliferation and is a prognostic indicator of poor survival. Mol Cancer. 2010; 9:221. [PubMed: 20727204]
39. Foster BA, Gingrich JR, Kwon ED, Madias C, Greenberg NM. Characterization of prostatic epithelial cell lines derived from transgenic adenocarcinoma of the mouse prostate (TRAMP) model. Cancer Res. 1997; 57:3325–30. [PubMed: 9269988]
40. Acosta JC, O'Loghlen A, Banito A, Raguz S, Gil J. Control of senescence by CXCR2 and its ligands. Cell Cycle. 2008; 7:2956–9. [PubMed: 18838863]
41. Kuilman T, Michaloglou C, Vredeveld LC, Douma S, van Doorn R, Desmet CJ, et al. Oncogene-induced senescence relayed by an interleukin-dependent inflammatory network. Cell. 2008; 133:1019–31. [PubMed: 18555778]
42. Yang J, van Oosten AL, Theunissen TW, Guo G, Silva JC, Smith A. Stat3 activation is limiting for reprogramming to ground state pluripotency. Cell Stem Cell. 2010; 7:319–28. [PubMed: 20804969]
43. Korkaya H, Kim GI, Davis A, Malik F, Henry NL, Ithimakin S, et al. Activation of an IL6 inflammatory loop mediates trastuzumab resistance in HER2+ breast cancer by expanding the cancer stem cell population. Mol Cell. 2012; 47:570–84. [PubMed: 22819326]
44. Wicha MS. PSA lo and behold: prostate cancer stem cells. Cell Stem Cell. 2012; 10:482–3. [PubMed: 22560068]
45. Qin J, Liu X, Laffin B, Chen X, Choy G, Jeter CR, et al. The PSA(−/lo) prostate cancer cell population harbors self-renewing long-term tumor-propagating cells that resist castration. Cell Stem Cell. 2012; 10:556–69. [PubMed: 22560078]
46. Dean M, Fojo T, Bates S. Tumour stem cells and drug resistance. Nat Rev Cancer. 2005; 5:275–84. [PubMed: 15803154]
47. Workman P. Inhibiting the phosphoinositide 3-kinase pathway for cancer treatment. Biochem Soc Trans. 2004; 32:393–6. [PubMed: 15046615]
48. Carver BS, Chapinski C, Wongvipat J, Hieronymus H, Chen Y, Chandarlapaty S, et al. Reciprocal feedback regulation of PI3K and androgen receptor signaling in PTEN-deficient prostate cancer. Cancer Cell. 2011; 19:575–86. [PubMed: 21575859]

Author Manuscript Author Manuscript Author Manuscript Author Manuscript

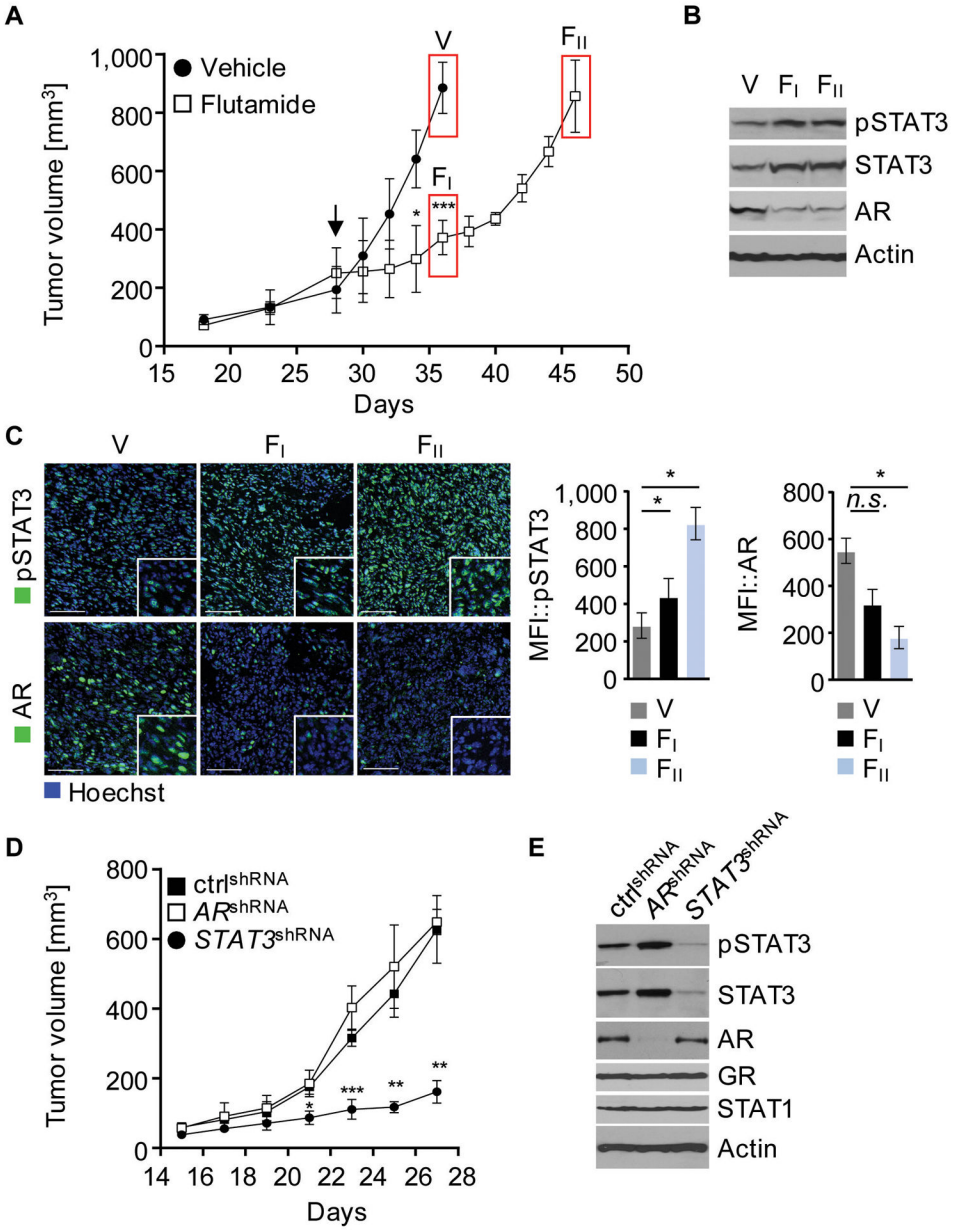

Figure 1. Downregulation of AR induces IL-6/STAT3 signaling

(A) Rag1−/− mice with subcutaneous (*s.c.*) TC1 tumors were treated with 25 mg/kg flutamide or vehicle control intraperitoneally (*i.p.*), every other day, starting 28 d after engraftment (arrow). Mean tumor volume are shown (n=6–7). Tumors were harvested 2 hours after last treatment (V, F_I, F_{II}). (B) Activated and total STAT3 is upregulated in tumors treated with flutamide. Western blot analysis with antibodies as indicated. (C) Tumor sections were prepared for immunofluorescence staining. Shown are representative confocal microscopy images and mean fluorescence intensities (MFI), (n=3); green, pSTAT3 (upper row), or AR (lower row); blue, nuclear staining with Hoechst. Scale bar, 100 μm. (D) TC1 cells expressing AR^{shRNA}, $STAT3^{shRNA}$, or non-silencing control (ctrl) shRNA injected in

Author Manuscript Author Manuscript Author Manuscript Author Manuscript

NSG/NOD mice. Tumors were harvested 27 days upon tumor engraftment. Results are presented as mean tumor volume (n=6). (E) Representative results of western blot analysis for tyrosine-phosphorylated or total STAT3, STAT1, AR, GR, and β-Actin are shown. (A, C, D) Error bars represent standard deviation; *n.s.* not significant, * $p < 0.05$, ** $p < 0.01$, *** $p < 0.001$.

Author Manuscript Author Manuscript Author Manuscript Author Manuscript

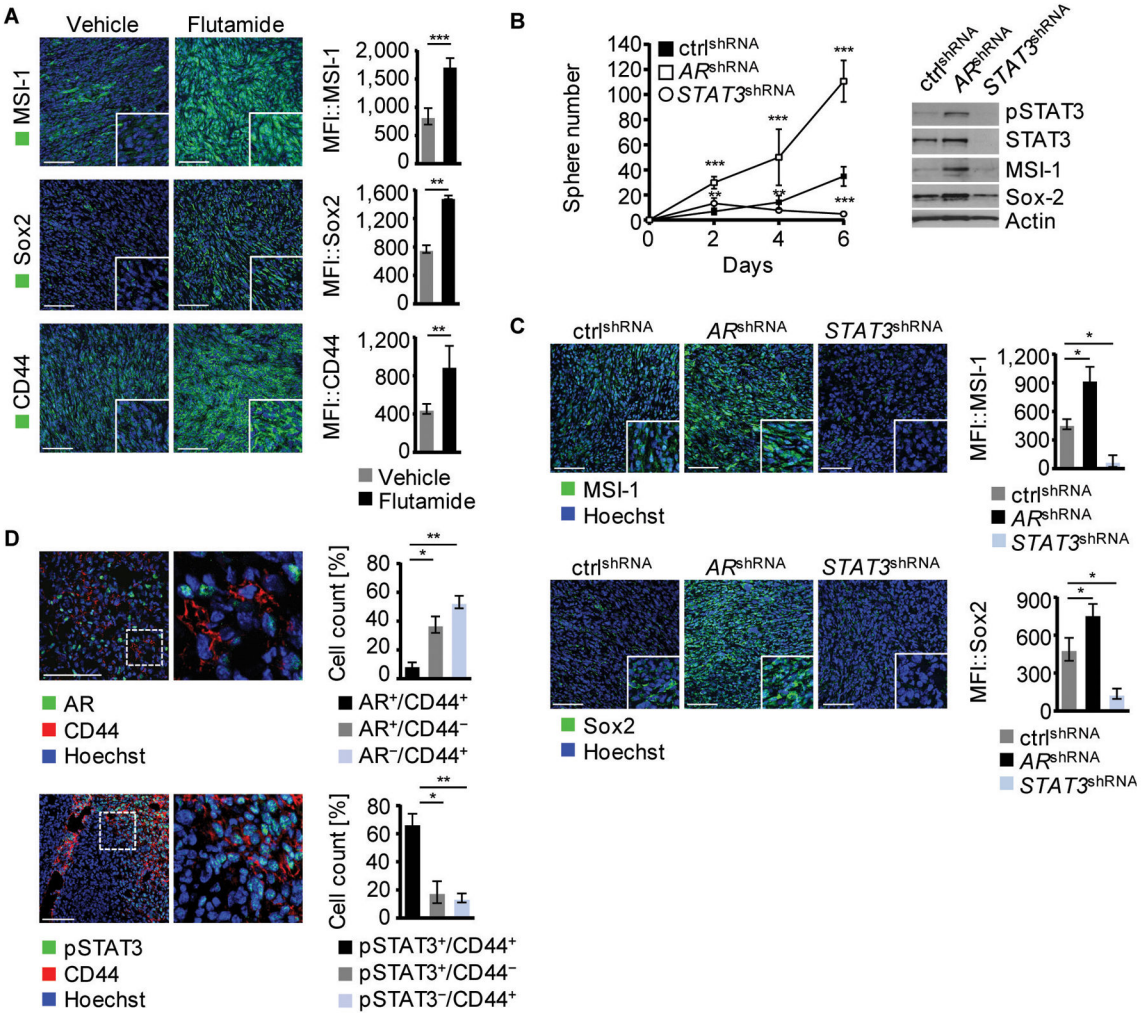

Figure 2. Cancer Stem Cell phenotype development is mediated by Stat3 but not AR

(A) Frozen sections from TC1 tumor-bearing mice treated with vehicle control or flutamide were stained for MSI-1, Sox-2, or CD44, green. Shown are representative immunofluoresceces (left) and mean fluorescence intensities (MFI) of 3 different tumors (right). Hoechst was used for nuclear staining, blue. (B) Shown is a tumor sphere formation assay of TC1 cells expressing AR^{shRNA}, $STAT3^{shRNA}$ or non-silencing control shRNA (n=7) (left). Western blot analysis with antibodies as indicated from TC1 tumor spheres (day 6) expressing AR^{shRNA}, $STAT3^{shRNA}$ or non-silencing control (right). (C) Immunofluorescence staining and mean fluorescence intensities (n=3) for MSI-1, and Sox2 of frozen tumor sections from mice injected with TC1 cells expressing AR^{shRNA}, $STAT3^{shRNA}$ or non-silencing control, nuclear staining: Hoechst. (D) Frozen sections of isolated TC1 tumors were stained for CD44 and AR or pSTAT3, Hoechst (blue). Double- and single- positive cells quantified (n=3). Scale bar: 100 μm. Standard deviation shown; *n.s.* not significant, * $p < 0.05$, ** $p < 0.01$, *** $p < 0.001$.

Author Manuscript Author Manuscript Author Manuscript Author Manuscript

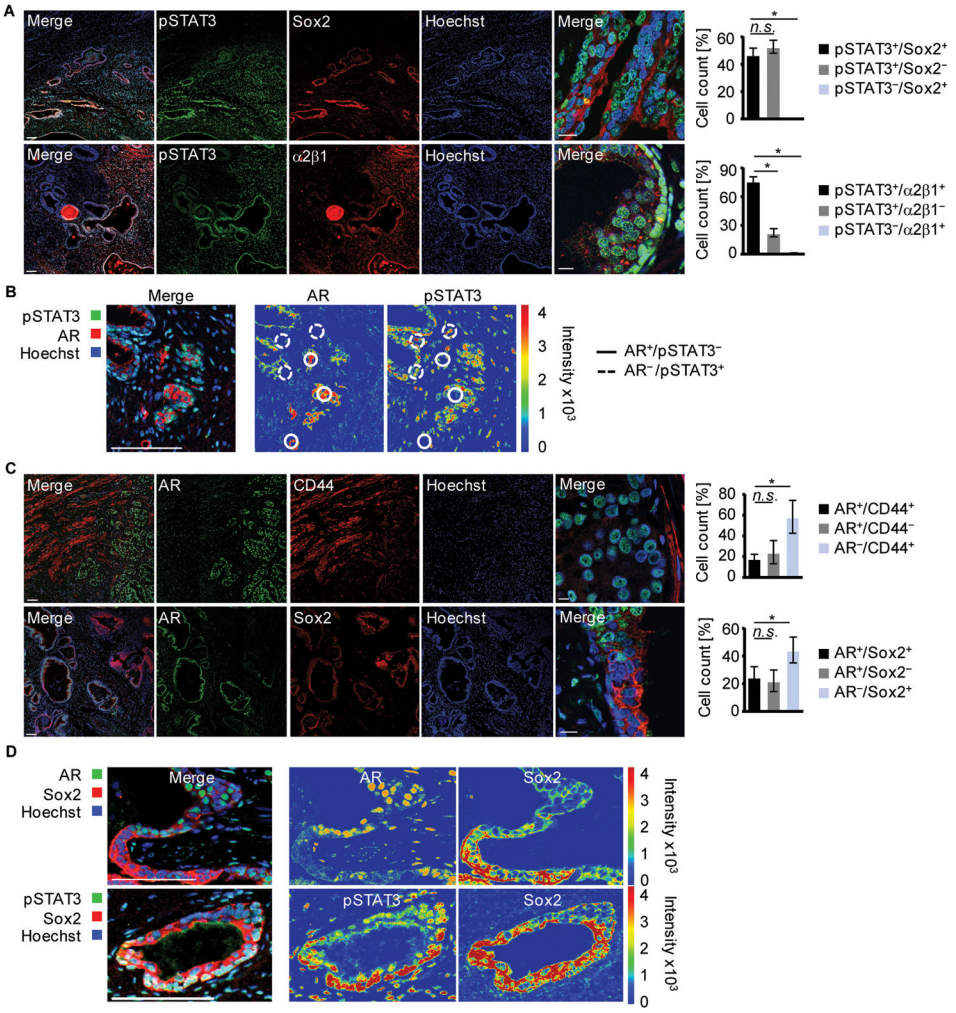

Figure 3. Low AR and high STAT3 activity in human prostate cancer samples

(A) Paraffin embedded slides of human PC tissue were stained for pSTAT3, and Sox2, or Integrin α2β1; nuclear staining with Hoechst. Scale bar 100 μm, 10 μm in magnifications (left). Single-positive and double-positive cells quantified (right). (B) Immunofluorescence of human PC tissue stained for pSTAT3 and AR; Hoechst was added for nuclear staining (left). Intensity-coded wrong color mode of pSTAT3 and AR is depicted (right). (C) Shown is a representative image of a human prostate cancer section stained for AR and CD44, or Sox2. Hoechst was used for nuclear staining (left). Double- and single- positive cells quantified (n=3), (right). (D) Detailed analysis of Sox2 and AR, or pSTAT3 stained tumor sections. Fluorescence intensities of AR, Sox2 and pSTAT3 are depicted in an intensity-coded wrong color mode as indicated; nuclear staining with Hoechst (blue). Sale bars: 100 μm, 10 μm in magnifications. Standard deviation shown; *n.s.* not significant, * $p < 0.05$, ** $p < 0.01$, *** $p < 0.001$.

Author Manuscript Author Manuscript Author Manuscript Author Manuscript

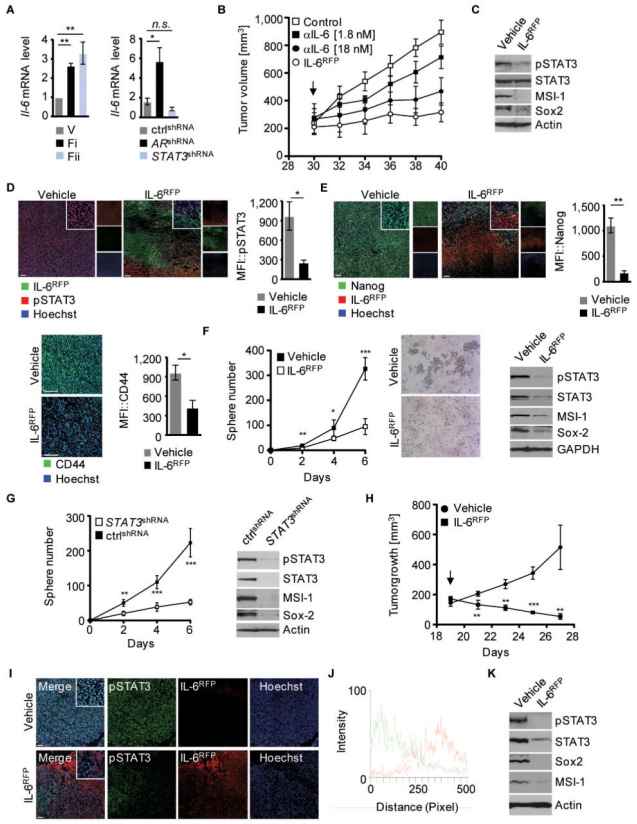

Figure 4. Decreased CSC phenotype education upon IL-6^{RFP} treatment

(A) Tumor homogenates of mice treated with either vehicle control or flutamide (left) or homogenates from engineered TC1 tumor cells as indicated (right) were prepared for RT-PCR. Bar graphs show fold inductions of IL-6 mRNA levels assessed in triplicate. (B) 30 days after tumor cell engraftment (arrow), TC1 tumor-bearing mice were treated with vehicle control (HEK^{CM}/IgG), 1.8 or 18 nM anti-IL-6 antibodies, or 1.8 nM IL-6^{RFP} twice daily. Mean tumor volumes shown (n=6). (C) Shown is a western blot from tumor homogenates of mice treated with vehicle or IL-6^{RFP}, detected with antibodies as indicated. (D) Immunofluorescences and MFIs (n=3) of tumor sections stained for pSTAT3 (red), His-tag (IL-6^{RFP}; green) and Hoechst (blue). (E) Immunofluorescent staining and MFIs for CD44 or Nanog (green), His-tag (IL-6^{RFP}; red); blue, Hoechst. MFIs of Nanog were measured in IL-6^{RFP} positive areas (n=3). (F) Tumor spheres of DU145 cells treated with vehicle or IL-6^{RFP} were quantified every other day (left). Spheres were imaged on day 6 (middle). Tumor spheres (day 6) were analyzed by western blot and detected with antibodies as indicated (right). (G) Tumor spheres of DU145 cells expressing STAT3^{shRNA} or non-silencing control shRNA were quantified every other day (left). Western blot analysis of tumorspheres with antibodies as indicated (right). (H) Nude mice with subcutaneous (*s.c.*) DU145 tumors were treated with 3.6 μg/kg IL-6^{RFP} or vehicle control peritumorally, starting 19 d after engraftment (arrow). Mean tumor volume shown (n=4). (I) Immunofluorescence staining of frozen tumor sections for pSTAT3, IL-6^{RFP} and Hoechst as indicated. (J) Fluorescence intensity profile of pSTAT3 (green) and IL-6^{RFP} (red) of IL-6^{RFP} treated mice from image shown in (I). (K) Tumors from mice treated with vehicle or IL-6^{RFP} were

analyzed by western blot, detected with antibodies as indicated. Scale bars: 100 μm. Error bars represent standard deviation; *n.s.* not significant, * $p < 0.05$, ** $p < 0.01$, *** $p < 0.001$.

Author Manuscript Author Manuscript Author Manuscript Author Manuscript

Author Manuscript Author Manuscript Author Manuscript Author Manuscript

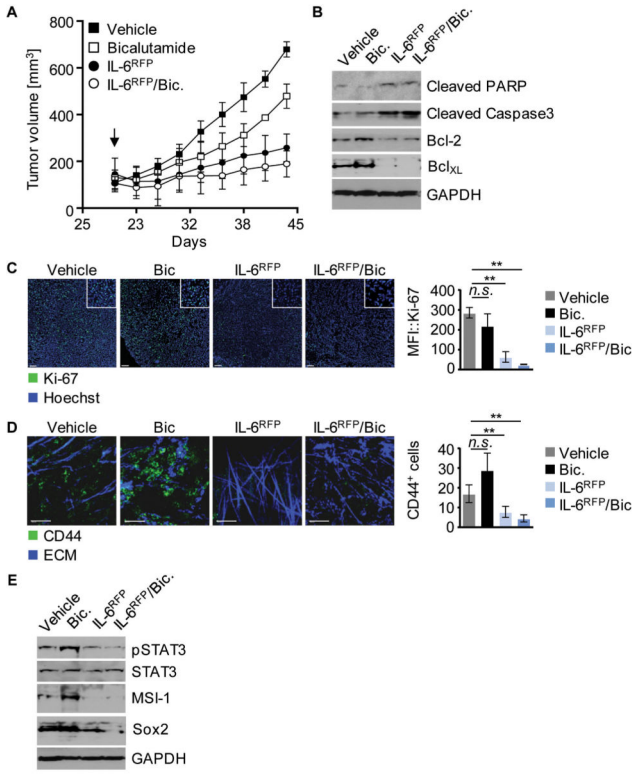

Figure 5. Impact of combined therapy using anti-androgen and IL-6^{RFP} on tumor growth

(A) Mice with subcutaneous (*s.c.*) TC1 tumors treated with vehicle control, 50 mg/kg bicalutamide (*i.p.*), 3.6 μg/kg IL-6^{RFP} (*s.c.*), or a combination of both. Injections of bicalutamide performed *i.p.* every other day. IL-6^{RFP} administered *s.c.* daily. Mean tumor volumes shown (n=6). (B) Western blot analysis of tumor lysates with antibodies as indicated. (C) Shown are immunofluorescences and MFIs of frozen tumor tissue stained for Ki-67; nuclear staining with Hoechst. Scale bar: 100 μm. (D) IVMPM on TC1-tumors 2 h after treatment as indicated. Green, CD44-FiTC; blue, ECM; Scale bar 200 μm. (E) Lysates from tumor tissue subjected to western blot and analyzed against pSTAT3, STAT3, MSI-1, Sox2, and GAPDH. Error bars represent standard deviation; *n.s.* not significant, * $p < 0.05$, ** $p < 0.01$, *** $p < 0.001$.